Section 5.6
Surveying, Mapping and GIS Techniques

3D Coastal Monitoring from very dense UAV-Based Photogrammetric Point Clouds

Fernando J. AGUILAR[1*], Ismael FERNÁNDEZ[2], Juan A. CASANOVA[3], Francisco J. RAMOS[3], Manuel A. AGUILAR[1], José L. BLANCO[1] and José C. MORENO[4]

[1] University of Almería, Departament of Engineering, Ctra. de Sacramento s/n, La Cañada de San Urbano, Almería 04120, Spain

[2] Servicios Técnicos NADIR S.L., C/ Cortina del Muelle 5, Málaga 29015, Spain

[3] SANDO S.A., Avda Ortega y Gasset 112.Málaga 29006, Spain

[4] University of Almería, Department of Informatics, Ctra. de Sacramento s/n, La Cañada de San Urbano, Almería 04120, Spain

* Corresponding author. Tel.: +34-950-015339; fax: +34-950-015491. E-mail address: faguilar@ual.es

Abstract In the present study, the potential use of unmanned aerial vehicles (UAVs) as a platform to flexibly obtain sequence of images along coastal areas from which producing high quality SfM-MVS based geospatial data is tested. A flight campaign was conducted over a coastal test site covering an area of around 4 has near Malaga (Spain). Images were taken on 1st December 2015 at a height above the ground ranging from 113.5 to 118 meters by using a Sony α6000® consumer camera mounted on a UFOCAM XXL v2® octocopter. 40 RTK-GPS surveyed ground points were evenly distributed over the whole working area. Furthermore, a very dense and accurate point cloud was collected by using a FARO Focus 3D X-130 terrestrial laser scanner (TLS). The photogrammetric block was computed by using two widely known SfM-MVS commercial software implementations such as Inpho UASMaster® and PhotoScan Professional®. PhotoScan provided a highly accurate bundle adjustment with errors of 1.5 cm, 1.5 cm and 6.1 cm along X, Y and Z axis respectively. The triangulation errors computed from UASMaster turned out to be slightly poorer along Z axis. In this sense, the very high resolution Surface Model built up from the corresponding photogrammetric point cloud depicted higher Z-differences with respect to the reference TLS derived surface model in the case of the UASMaster workflow. Summing up, the high degree of automation and efficient data acquisition provided by UAV-based digital photogrammetry makes this approach competitive and useful to be applied in high resolution 3D coastal mapping.

Keywords: SfM-MVS; UAV; Photogrammetric point cloud; Coastal monitoring; 3D coastal mapping.

B. Eynard et al. (eds.), *Advances on Mechanics, Design Engineering and Manufacturing*, Lecture Notes in Mechanical Engineering,
DOI 10.1007/978-3-319-45781-9_88

1 Introduction

Mediterranean coastal areas are being progressively degraded mainly because they are withstanding a high pressure linked to an increasing economic activity that provides large profits from the tourist industry. This process is causing the emergence of new infrastructures (harbors, roads, urbanizations, engineered structures, etc.) which are seriously affecting coastal environment [1]. In this sense, it is worth noting that urban development of coastal areas and resource use conflicts spawn environmental degradation and increasing hazard vulnerability [2]. As a result, some specific programs have been developed for the Mediterranean Sea (*e.g.* United Nations Environment Program/Mediterranean Action Plan) in order to study the degradation and conservation processes along Mediterranean coastal areas.

Among the coastal environments, sandy beaches constitute the most dynamic natural system as well as the most exposed to morphological variations. Furthermore, they are usually under a large anthropic influence. Sandy beaches behave differently regarding the spatial and temporal scales. On one hand, seasonal changes along shoreline cross-profiles may be observed from winter to summer and also due to specific atmospheric events such as storms surge [3]. On the other hand, the general trend of coastal evolution can be assessed by means of a long-term evolution study [4].

Historically, the shoreline has been used as the main indicator of the coastal dynamic [4, 5]. Hence the geomatics techniques utilized for its extraction have been extended to a wide set of fields such as researching, engineering, management, land-use planning and environmental issues. Notice that long coastlines and dynamic processes make the application of traditional surveying difficult, but recent advances made in the geomatics discipline allow for more effective methodologies to be investigated.

The development of some techniques that make possible to efficiently obtain high accuracy Digital Surface Models (DSM), such as Digital Aerial Photogrammetry or airborne LiDAR technology, have pointed out to the datum-coordinated shorelines, based on either tidal or vertical reference datums, as the most suitable shoreline indicator [5], since a shoreline extracted from a stable vertical datum can be treated as a reference shoreline and used to accurately compute shoreline change rates at local scale so allowing the reliable simulation of coastal erosion. Moreover, coastal geomorphology requires accurate topographic data of the so-called beach systems to carry out a number of simulations related to flooding phenomena and assessment of the coastal sediment budget [6]. In this way, the emergence of Structure from Motion (SfM) with Multi-View Stereo (MVS) in recent years has revolutionized 3D topographic surveys by significantly boosting efficiency in collecting and processing data. Coming from the fields of computer vision and photogrammetry, SfM-MVS can produce, under certain conditions, very dense and accurate 3D point clouds of comparable quality to existing laser-based

methods (*e.g.* Airborne Laser Scanning (ALS) or even Terrestrial Laser Scanning (TLS)) [7]. In fact, the image-based approach [8], supported by recent developments in computer vision [9], is helping to provide additional automated methods for both image orientation and 3D reconstruction at different scales [10].

The main goal of the present study was to test the potential use of unmanned aerial vehicles (UAVs) as a platform to flexibly obtain sequence of images along coastal areas from which efficiently producing high quality and dense SfM-MVS based geospatial data.

2 Study site and dataset

An UAV-based flight campaign was conducted over a coastal test site covering a target area of around 4 has near the city of Málaga, located at south of Spain (Figure 1). The working area consisted of a sandy Mediterranean beach (foreshore) and a shrubland zone (backshore). The flight pattern consisted of three strips composed of 97 vertical (nadir) images with a forward and side overlap of 90% and 50% respectively.

Fig 1. Location of the coastal study site.

Images were taken on 1st December 2015 at a height above the ground ranging from 113.5 to 118 meters by using a Sony α6000® consumer camera mounted on a UFOCAM XXL v2® octocopter whose acquisition rate was automatically set on one shot per second. The high redundant set of images acquired facilitated the application of SfM-MVS approach. The camera, equipped with a 24.3 megapixel APS-C CMOS sensor (4.19 μm/pixel), was set at 30 mm focal length, therefore capturing RGB images at approximately 1.5 cm Ground Sample Distance (GSD). 40 ground points, constituted of different targets (marks painted on the ground, artificial targets, etc.), were evenly distributed over the whole working area and surveyed by applying Real Time Kinematic (RTK) GPS technique from using a couple of base and rover Trimble R6 receivers (Figure 2).

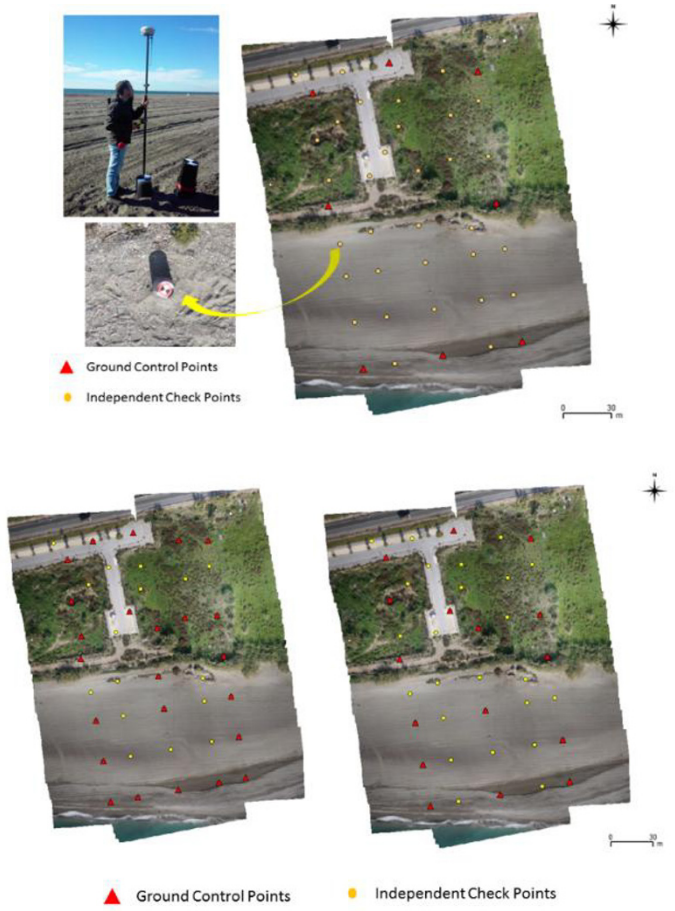

Fig 2. Orthomosaic (GSD = 2 cm) depicting ground points distribution and artificial targets. 8 (top), 24 (bottom-left) and 16 (bottom-right) GCPs configurations.

A range from 8 to 24 ground points (Figure 2) were employed as Ground Control Points (GCPs) manually marked on the digital images to carry out the triangulation and bundle adjustment process to obtain the external orientation parameters for each photogram belonging to the photogrammetric block. It allowed the transformation of the structure-from-motion point cloud into real world coordinates (UTM 30N ETRS89 and orthometric heights EGM08 REDNAP). They were also used to carry out a camera self-calibration process, except focal length (fixed at 30 mm), headed up to optimize the camera model (principal point offset and radial and tangential distortion). The remaining ground points were used as independent check points (ICPs) for assessing the 3D accuracy of the bundle adjustment. A very dense and accurate point cloud, representing a proper ground truth for com-

parison purposes, was also obtained by co-registering four independent point clouds collected through a FARO Focus 3D X-130 terrestrial laser scanner (TLS). This reference TLS point cloud was georeferenced by applying a 3D conformal coordinate transformation based on the surveyed RTK-GPS world coordinates of 6 spheres evenly located over the whole working area. Finally, the photogrammetric block was computed in the same way but using two SfM-MVS commercial software implementations such as Inpho UASMaster® and PhotoScan Professional®.

3 Results and discussion

Regarding the photogrammetric triangulation accuracy assessment results, computed at ICPs and working on only 8 GCPs evenly distributed over the test site (corners and sides of the photogrammetric block. Please see Figure 2, top), PhotoScan software provided a highly accurate bundle adjustment with errors (measured as root mean square error or rmse) of 1.5 cm, 1.5 cm and 6.1 cm along X, Y and Z axis respectively. The triangulation errors computed from UASMaster bundle adjustment turned out to be slightly poorer along Z axis, with $rmse_z$ = 10.6 cm, performing very similar with respect to planimetric accuracy ($rmse_x$ = 1.3 cm and $rmse_y$ = 1.6 cm). Table 1 depicts that the residuals of the bundle adjustment transformation measured at ICPs decreased when increasing the number of GCPs. The accuracy results at this first stage (SfM phase) between PhotoScan and UASMaster turned out to be quite similar only when the number of GCPs was equal or higher than 16 GCPs. Note that the output of the SfM stage is a sparse and unscaled 3D point cloud in arbitrary units along with camera models and poses. At least three GCPs with XYZ coordinates are needed to scale and georeference the SfM-derived point cloud by means of a seven parameter linear similarity transformation [11]. Therefore, and unlike conventional photogrammetry, each photograph does not require to contain visible GCPs. Nowadays, it is even possible to undertake the so-called "direct" georeferencing, so avoiding photogrammetric ground control, through known attitude and camera positions given by RTK-GPS measurements and an Inertial Measurement Unit [12].

Table 1. Accuracy results computed at the Ground Points not used in the photogrammetric bundle adjustment computation (32, 24 and 16 independent check points respectively).

		$rmse_x$ (cm)	$rmse_y$ (cm)	$rmse_z$ (cm)
8 GCPs	PhotoScan®	1.5	1.5	6.1
	UASMaster®	1.3	1.6	10.6
16 GCPs	PhotoScan®	1.2	1.2	3.7
	UASMaster®	1.1	0.9	3.9
24 GCPs	PhotoScan®	1.2	1.0	3.4
	UASMaster®	1.2	0.9	3.8

With regards to the second stage, that is point cloud densification or MVS phase, which is very related to 3D surface reconstruction, MVS algorithms usually increase the density of the initially sparse point cloud by at least two orders of magnitude applying, among other approaches, depth-maps merging methods [7].

Table 2. Vertical accuracy results computed at N = 2041997 points for the digital surface models (5 cm grid spacing) provided by the SfM-MSV commercial software implementations tested.

		Z-differences (cm) TLS – PhotoScan	Z-differences (cm) TLS – UASMaster
8 GCPs	Mean error	-1.5	-11.0
	Median	-1.5	-8.8
	Standard Deviation	4.1	9.0
16 GCPs	Mean error	-3.3	-1.0
	Median	-3.1	1.5
	Standard Deviation	3.1	8.8
24 GCPs	Mean error	-2.7	-1.6
	Median	-2.3	0.7
	Standard Deviation	3.1	8.8

The very high resolution DSM built up from the corresponding photogrammetric point cloud (5 cm grid spacing), strictly computed over the sandy beach land cover and only using eight GCPs , depicted higher Z-differences with respect to the reference TLS derived surface model (ground truth) in the case of UASMaster workflow, providing a non-negligible systematic error of -11 cm (given as the mean of $Z_{TLS} - Z_{UASMaster}$ differences) and a random error, measured as standard deviation, of 9 cm (Table 2). Notice that, on the contrary, the mean error computed for the Z-differences between TLS data and PhotoScan derived DSM took a value of -1.5 cm, also presenting a standard deviation of 4.1 cm significantly lower than that calculated in the case of UASMaster (Table 1). Furthermore, the standard deviation of Z-differences remained fairly steady when increasing the number of GCPs on which the photogrammetric block was computed (SfM stage) in the case of UASMaster approach. In this sense, there was little improvement from adding more GCPs to compute the photogrammetric triangulation and the initial sparse point cloud regarding random error. Yet, systematic error was clearly lowered after increasing the number of GCPs constraining the photogrammetric block. PhotoScan software performed better and showed more stable vertical error regardless the number of GCPs used to adjust the photogrammetric block.

The corresponding histograms of Z-differences, given as TLS minus photogrammetrically derived point cloud, both for the case of PhotoScan and UASMaster and eight GCPs, are shown in Figure 3. It is important to highlight that PhotoScan vertical residuals fitted better a Gaussian distribution (overlaid on

the histogram) than UASMaster ones, proving the better performance of the MVS algorithm implemented in PhotoScan software. This finding was clearly corroborated by plotting the 2D spatial distribution of residuals (Figure 4), where a sharp mosaicked effect can be made out in the case of the UASMaster-derived DSM.

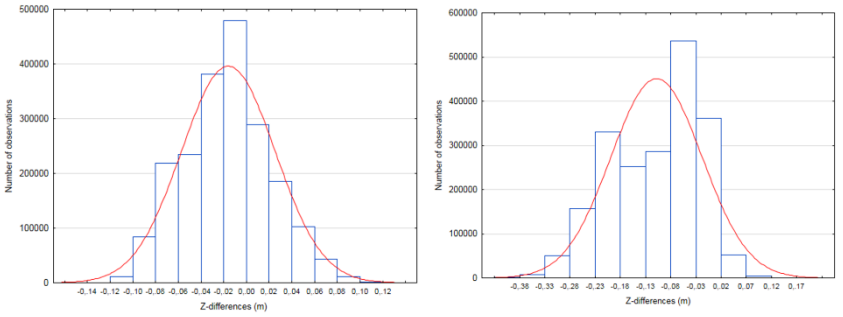

Fig 3. Histogram of Z-differences within the sandy beach land cover between TLS point cloud minus PhotoScan-derived DSM (left) and UASMaster-derived DSM (right) (5 cm grid spacing).

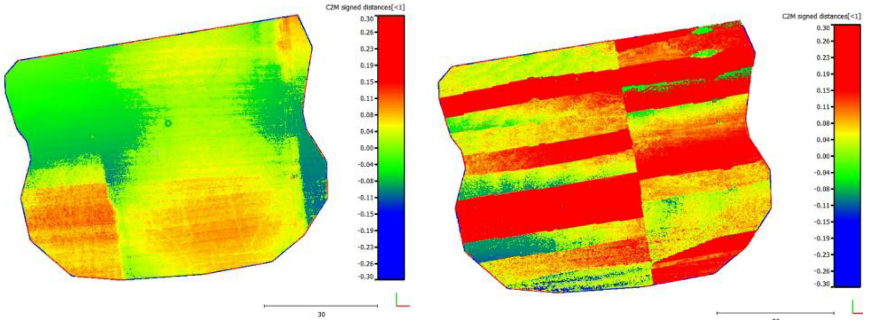

Fig 4. Z-differences (meters) within the sandy beach land cover given as PhotoScan (left) and UASMaster (right) point cloud (both based on eight GCPs) minus TLS point cloud.

4 Conclusions

The approach proposed in this work integrates Structure-from-Motion (SfM) and Multiview-Stereo (MVS) algorithms and, in contrast to traditional photogrammetry techniques, it requires little expertise, few control measurements and, moreover, processing is practically automated. Although the absolute accuracy of TLS point clouds is superior to SfM-MVS photogrammetry when working over a range of several meters, the high degree of automation and efficient data acquisition provided by UAV-based SfM-MVS digital photogrammetry makes this approach

extremely competitive and useful to be applied in high resolution 3D coastal mapping. It is worth noting that the quasi-flat surface surveyed in this work would not be the best 3D surface to perform camera auto-calibration. In this sense, a preflight camera calibration would be required in order to improve the current results by accurately modeling the inner camera geometry.

Among other added-value geospatial products provided by SfM-MVS, we can highlight the 3D photorealistic models made up of high quality 3D textured triangular meshes ready to be 3D printed or inserted in 3D immersive environments.

Acknowledgments The research work reported here was made possible through the research project 3DCOAST, funded by "Corporación Tecnológica de Andalucía" (Regional Government of Andalusia) and the Spanish company SANDO S.A. It takes part of the Internacional Campus CEIMAR and the 3DLAB research lines (UNAM13-1E-1191 Spanish Government).

References

1. Suárez de Vivero J.L. and Rodríguez Mateos J.C. Coastal crisis: The failure of coastal management in the Spanish Mediteranean region. Coastal Management, 2005, 33(2), 197-214.
2. Mills J.P. Buckley S.J. Mitchell H.L. Clarke P.J. and Edwards S.J. A geomatics data integration technique for coastal change monitoring. Earth Surface Processes and Landforms, 2005, 30(6), 651-664.
3. Hernández L. Alonso, I. Sánchez-Pérez I. Alcántara-Carrió J. and Montesdeoca I. 2007, Shortage of sediments in the Maspalomas dune field (Gran Canaria, Canary Islands) deduced from analysis of aerial photographs, foraminiferal content, and sediment transport trends. Journal of Coastal Research, 2007, 23(4), 993-999.
4. Douglas B.C. and Crowell M. Long-term shoreline position prediction and error propagation. Journal of Coastal Research, 2000, 16(1), 145-152.
4. Moore L.J. Shoreline mapping techniques. Journal of Coastal Research, 2000, 16(1), 111-124.
5. Fernández I. Aguilar F.J. Aguilar M.A. Pérez J. and Arenas A. A new, robust, and accurate method to extract tide-coordinated shorelines from coastal elevation models. Journal of Coastal Research, 2012, 28(3), 683-699.
6. Mancini F. Dubbini M. Gattelli M. Stecchi F. Fabbri S. and Gabbianelli G. Using unmanned aerial vehicles (UAV) for high-resolution reconstruction of topography: the structure from motion approach on coastal environments. Remote Sensing, 5, 2013, pp.6880-6898.
7. Smith M.W. Carrivick J.L. and Quincey D.J. Structure from motion photogrammetry in physical geography. Progress in Physical Geography, 2016, 40(2), 247-275.
8. Remondino F. and El-Hakim S. Image-based 3D modelling: a review. Photogrammetric Record, 2006, 21(115), 269-291.
9. Furukawa Y. and Ponce J. Accurate dense and robust multiview stereopsis. IEEE Transactions on Pattern Analysis and Machine Intelligence, 2010, 32(8), 1362-1376.
10. Remondino F. Grazia M. Nocerino E. Menna F. and Nex F. State of the art in high density image matching. Photogrammetric Record, 2014, 29(146), 144-166.
11. James MR and Robson S. Straightforward reconstruction of 3D surfaces and topography with a camera: Accuracy and geoscience application. Journal of Geophysical Research: Earth Surface, 2012, 117(F03017), doi:10.1029/2011JF002289.
12. Colomina I. Molina P. Unmanned aerial system for photogrammetry and remote sensing. ISPRS Journal of Photogrammetry and Remote Sensing, 2014, 92, pp. 79-97.